

NEW CRATER SIZE-FREQUENCY DISTRIBUTION MEASUREMENTS OF THE APOLLO 16 LANDING SITE. T. Gebbing¹, H. Hiesinger¹, W. Iqbal¹ and C. H. van der Bogert¹, ¹Institut für Planetologie, Westfälische Wilhelms-Universität, Wilhelm-Klemm-Str. 10, 48149, Münster, Germany, (thorsten.gebbing@uni-muenster.de).

Introduction: Crater size-frequency distribution (CSFD) measurements are used in conjunction with the lunar chronology to determine model ages of geological units on terrestrial bodies across the Solar System [1-8]. The chronology is based on connecting sample ages to the cumulative number of craters observed on geological units representative of the samples [4-9]. Using recent data from the Lunar Reconnaissance Orbiter Camera (LROC) and SELENE/Kaguya Terrain Camera, we reexamine and improve the calibration for the Apollo 16 landing site by (1) counting the areas of [2,3] on the new data, and (2) comparing these results with CSFDs of improved count areas. Here, we report the new CSFDs, $N(1)$ values, and absolute model ages (AMAs) from around the Apollo 16 landing site.

Apollo 16 Landing Site: The Apollo 16 landing site is located in the Descartes Highlands, specifically in the Cayley formation between North Ray and South Ray craters, about 140 km southwest of the Alfraganus crater [10]. The original count areas of [2] are located in the Cayley formation: (1) to the northwest inside Dollond B crater, (2) to the northeast, and (3) at the Apollo 16 landing site itself (red areas, Fig. 1). The collected samples are primarily breccias with radiometric ages between 3.4 and ~3.8 Ga [11].

Methods: LRO Wide Angle Camera (WAC) and Kaguya images were processed using the Integrated Software for Imagers and Spectrometers (ISIS) [12] and imported into ArcGIS. The count areas and crater measurements were done with CraterTools [13] in ArcMap. First, we did the confirmation measurements on the areas of [2,3] (Fig. 1, red areas). Next, we improved the definition of the areas where noticeable geological and topographical boundaries were observed using morphological and albedo contrast, Clementine spectral data, and the WAC digital terrain model. Then, we measured the CSFDs in the updated areas (Fig. 1, blue areas), and in some areas which differ in appearance within these plains area (Fig. 1, white areas). Noticeable secondary craters were marked and excluded, and randomness analysis [14] was used to identify and exclude additional crater clustering. The CSFDs were imported into Craterstats 2.0 and plotted in cumulative and relative forms [15,16] using the production function of [4] to derive absolute model ages (AMAs) (Fig. 2).

Results and Discussion: The previously determined $N(1)$ values for the three red count areas (Fig. 1) were $3.4 \pm 0.7 \times 10^{-2} \text{ km}^{-2}$ [3] and $2.490 \times 10^{-2} \text{ km}^{-2}$ to

$2.509 \times 10^{-2} \text{ km}^{-2}$ [17]. For the recounted areas (Fig. 1 (a), 1-3) we got an $N(1)$ of $1.84 \times 10^{-2} \text{ km}^{-2}$ and for the updated blue areas (Fig. 1 (b), 4-6) $N(1) = 1.88 \times 10^{-2}$

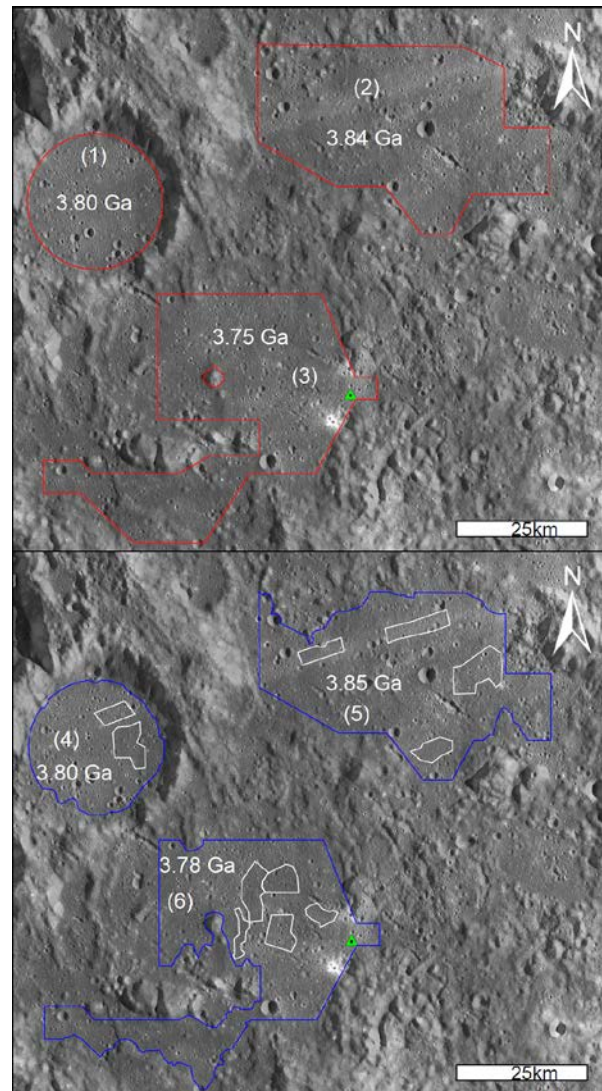


Figure 1. Count areas around the Apollo 16 landing site (green triangle). (a) Red boundaries mark the count areas of [2] for the calibration of the lunar cratering chronology, for which we recounted and refit the AMAs (white numbers). (b) Blue boundaries mark the improved counting areas, that were measured using LRO-WAC and Kaguya images. The results of both crater counts on WAC images are similar and correspond with previous results from [3,5]. The white areas mark the units counted on Kaguya data.

Table 1. $N(1)$ s and AMAs of the six recounted areas of [2] around the Apollo 16 landing site. The fifth and last line represents the combined three areas their $N(1)$ and age, which are used in the discussion.

Unit	$N(1)$ (km^{-2})	AMA (Ga)
1	1.79×10^{-2}	3.80 ± 0.02
2	2.27×10^{-2}	3.84 ± 0.02
3	1.35×10^{-2}	3.75 ± 0.02
1 - 3	1.84×10^{-2}	3.80 ± 0.02
4	1.76×10^{-2}	3.80 ± 0.02
5	2.42×10^{-2}	3.85 ± 0.02
6	1.38×10^{-2}	3.78 ± 0.02
4 - 6	1.88×10^{-2}	3.81 ± 0.02

km^{-2} . For comparison, [5] determined an $N(1)$ of $3.1 \pm 0.3 \times 10^{-2} \text{ km}^{-2}$. The AMAs of [3] are $3.9 \pm 0.1 \text{ Ga}$, while our newly determined ages are $3.80 \pm 0.02 \text{ Ga}$ and $3.81 \pm 0.02 \text{ Ga}$ (shown in Fig. 2). While these AMAs are similar, the smaller areas (Fig. 1 (b), white) show younger ages. The $N(1)$ values are $5.35 \times 10^{-2} \text{ km}^{-2}$ to $1.66 \times 10^{-2} \text{ km}^{-2}$, with AMAs from 3.53 ± 0.09 to $3.79 \pm 0.07 \text{ Ga}$.

Our results (Table 1) for both the recounted and the updated areas give $N(1)$ and AMA values which are within the error of [2] and [3], and are comparable to those of [5]. In contrast to this are the smaller areas, which show younger ages, possibly due to their sampling more recent local geological activity [e.g., 18,19]. To investigate these effects, the areas will be expanded and counted on both the LRO-NAC and Kaguya data.

Outlook: Further CSFD measurements are ongoing in combination with the production of a new geological map of the Apollo 16 region. The map and CSFD measurements will be combined to provide an updated and improved assessment of the Apollo 16 lunar cratering chronology calibration points [e.g., 8].

Acknowledgement: CvdB was supported by EU H2020 project #776276, PLANMAP.

References: [1] Hartmann (1970) *Icarus* 13, 299-301. [2] Neukum et al. (1975) *The Moon* 12, 201-229. [3] Neukum (1983) *Habil. thesis, U. of Munich*. [4] Neukum et al. (2001) *Space Sci. Reviews* 96, 55-86. [5] Robbins (2014) *Earth and Planet. Sci. Lett.* 403, 188-198. [6] Stöffler et al. (2006) *Reviews in Mineral. & Geochem.* 60, 519-596. [7] Hiesinger et al. (2000) *JGR* 105, 29239-29275. [8] Hiesinger et al. (2012) *JGR* 11, E00H10. [9] Hiesinger et al. (2015) *LPSC* 46, #1834. [10] Ulrich et al. (1981) *USGS Report* 1048. [11] Joy et al. (2011) *GCA* 75, 7208-7225. [12] Anderson et al. (2004) *LPSC* 35, #2039. [13] Kneissl et al. (2011). *PSS* 59, 1243-1254. [14] Michael et al. (2012) *Icarus* 218, 169-177. [15] Michael et al. (2016) *Icarus* 277, 279-285. [16] Michael et al. (2010) *EPSL* 294, 223-229. [17] Marchi et al. (2009) *AJ* 137, 4936-4948. [18] Pasckert et al. (2015) *Icarus* 257, 336-354. [19] van der Bogert et al. (2015) *Wksp on Crater Statistics*, 9023.

Figure 2. CSFD measurement of the updated area representative of the Apollo 16 landing site [2] counted on WAC data. Combined CSFD distribution of the three edited count areas in a cumulative fit (a) with the determined absolute model age. Shown above is the randomness analysis of the WAC count area and in (b) the relative crater frequency plot.

